DNA Constraints Allow Rational Control of Macromolecular Conformation

Chandrasekhar V. Miduturu and Scott K. Silverman*

Department of Chemistry, University of Illinois at Urbana-Champaign, 600 South Mathews Avenue, Urbana, Illinois 61801

Context of the New Experiments Within DNA Nanotechnology. Most efforts within DNA nanotechnology can be classified with respect to two descriptors, for $2 \times 2 = 4$ possible combinations (Fig. S1). First, a DNA nanotechnology experiment may be classified with respect to whether the DNA is "static" or "dynamic" after its assembly at the start of the experiment. Second, an experiment may be classified according to whether DNA alone is used or whether other objects such as RNA, proteins, or nanoparticles are involved. Examples of three of the four possible combinations of these descriptors have been reported, with key examples cited in Fig. S1. In all of these previous efforts, no unambiguous example of "dynamic DNA/involves other objects" DNA nanotechnology has been described. In particular, our current report describes the first example of direct, *dynamic* DNA control over the conformation of *another molecule*. A key feature of our experimental design is that formation of double-helical DNA and adoption of native higher-order structure by the macromolecule are in direct competition, as illustrated schematically in Fig. 1A and with molecular models in Fig. 1B. We emphasize that in these experiments, we are not seeking the creation of ordered (either periodic or aperiodic) arrays of other molecules on a DNA scaffold, as has been done in many of the other efforts. We are also not seeking the spatial organization of intact macromolecules without affecting their conformations. In this initial study, we have used RNA as the test system for conformational control using DNA constraints. We anticipate that other macromolecules such as proteins should be amenable to the approach as well.

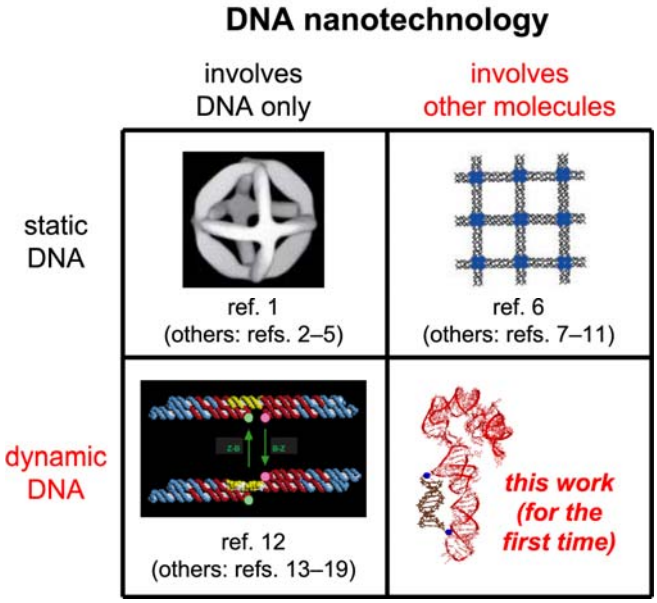

Figure S1. Context of the new experiments within DNA nanotechnology.

Depiction of the DNA Constraint Strategy. Fig. 1 shows an abbreviated illustration of the strategy for controlling RNA conformation with a DNA constraint. Fig. S2 shows an expanded depiction of this strategy. The Mg^{2+}-dependent folding of the RNA and the formation of duplex DNA contribute to coupled equilibria. To first order, duplex DNA formation is independent of Mg^{2+}, because Watson-Crick base pairing does not require this metal ion. Therefore, the Mg^{2+} concentration controls the balance between RNA folding and duplex DNA formation for any particular RNA-DNA conjugate. At low Mg^{2+} concentration (*top row* in Fig. S2), the folded RNA conformation (*green*) is unstable without Mg^{2+}, and therefore the RNA misfolds (*red*), whereas the duplex DNA constraint (*brown*) is intact (note the position of equilibrium). Even without the DNA, the RNA would not fold properly in the absence of Mg^{2+}, because Mg^{2+} is required for RNA structure.[20] However, when Mg^{2+} is present (*bottom row*), the folded RNA conformation is stabilized by tertiary contacts (*dotted lines*) that inherently require Mg^{2+} (*orange spheres*). If sufficient Mg^{2+} is added and if enough energy is gained upon folding the RNA, then the duplex DNA constraint is disrupted, and the equilibrium lies toward the folded RNA. Note that the DNA strands do not necessarily need to dissociate completely for sufficient disruption of the constraint, although full dissociation is depicted here for clarity. The destabilization of RNA folding by an incompatible DNA constraint is manifested empirically in a higher Mg^{2+} requirement for RNA folding. The increased Mg^{2+} requirement (e.g., Fig. 2) is correlated quantitatively with the energetic penalty for disrupting the DNA constraint, using equations that were described previously.[21]

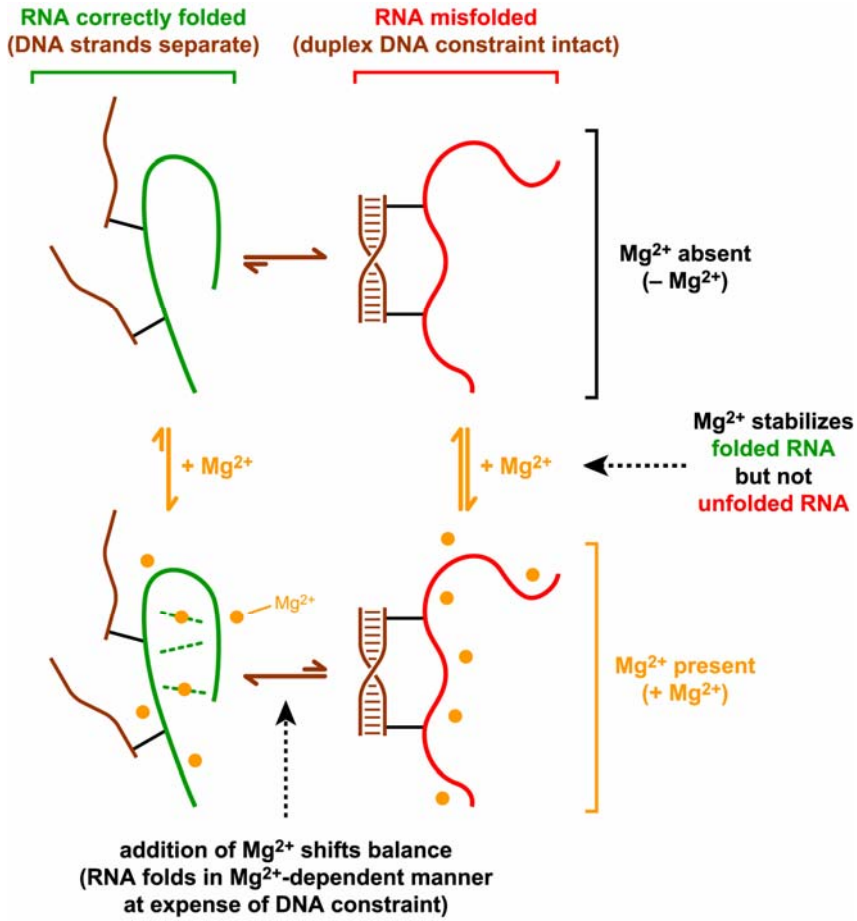

Figure S2. Expanded depiction of the strategy by which a DNA constraint controls macromolecular RNA structure.

Computer Modeling of Nucleic Acid Structures. The misfolded P4-P6 RNA conformation shown in Fig. 1B (*red*) depicts one possible misfolded state of the DNA-constrained RNA, although many other misfolded states are possible. In a three-step procedure, this misfolded conformation was modeled using MOE (Chemical Computing Group, Montreal), version 2004.3.

(1) The PDB structure of the P4-P6 RNA (PDB id 1GID, molecule B) was imported and hydrogen atoms were added. The structure was energy-minimized using the AMBER94 force field with a non-bonded cutoff for van der Waals and electrostatic interactions between 8–10 Å. No explicit solvation or counterions were included, and a distant-dependent dielectric was used to include solvation effects implicitly. The energy minimization was continued until the root-mean-square gradient of the energy was <0.05 kcal/mol/Å.

(2) A 10-bp B-form DNA duplex was created using the "create sequence" function. At both ends of the duplex, the 5'-thymidine nucleotide was covalently linked with the appropriate RNA 2'-amino group using the connection shown in Scheme 1. In the computer model, the DNA was initially placed as close as possible to the RNA while ensuring that no steric clashes were present. Nucleotides A113-A207 of the RNA were deleted, and the structure was minimized as above with all of the DNA fixed except for the 5'-terminal CH_2O moiety of each strand.

(3) The A113–A207 RNA fragment was re-introduced and manually positioned approximately as shown in Fig. 1B. The G112-A113 and A207-C208 phosphodiester linkages were restored, and the entire structure was minimized with RNA nucleotides 102-111 and 209-261 and all of the DNA fixed (only the A113–A207 RNA fragment plus C208 and G112 were allowed to move). Finally, the entire structure was minimized with all of the DNA fixed.

Separately, the 10-bp and 20-bp DNA constraints were modeled with the RNA fixed; the results are shown in Fig. S3. Due to the geometrical mismatch, the 10-bp DNA constraint must distort if the RNA conformation is maintained. In practice, experimental data indicate that the 10-bp DNA duplex is retained and the RNA itself misfolds, resulting in a higher Mg^{2+} requirement for RNA folding (Fig. 2, *red triangles*). In contrast, the 20-bp DNA constraint is compatible with the RNA conformation, and no RNA misfolding is predicted. Indeed, the Mg^{2+} requirement for folding with the 20-bp duplex is nearly equivalent to that of unconstrained P4-P6 (Fig. 2, *green squares*).

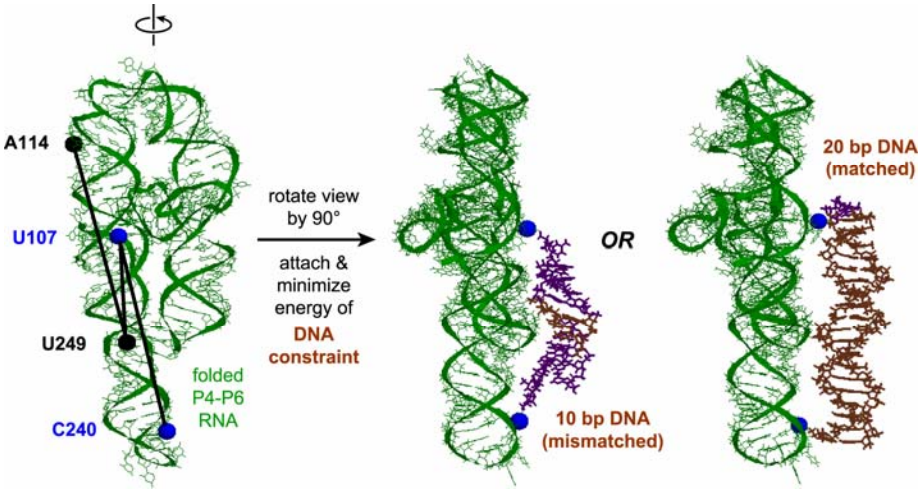

Figure S3. Modeling of DNA-constrained P4-P6 RNA with the RNA (*green*) fixed in its native conformation. The DNA constraints are colored brown for standard B-form duplex regions and purple for distorted regions.

General Experimental Considerations. Standard DNA oligonucleotides were prepared by solid-phase synthesis at Integrated DNA Technologies (Coralville, IA). DNA oligonucleotides incorporating a 5'-modified phosphoramidite (Fig. S4A) as well as all RNA oligonucleotides were prepared by solid-phase synthesis at the UIUC W. M. Keck Center. Transcription of P4-P6 RNA sequences used T7 RNA polymerase and a linearized plasmid DNA template.[22] The plasmids encoding P4-P6-wt (nt 102-261), P4-P6-bp (nt 102-261 with nt 123-126 ACAG in the J5/5a joining region[23,24] replaced with UGU), and Δ15-P4-P6 (nt 117-261; fragments **II**+**III** of Fig. S4B in both wt and bp versions) were available from a previous study.[22] The plasmid encoding P4-P6 nt 117-237 terminating with a 2',3'-cyclic phosphate via a co-transcriptional hammerhead ribozyme (fragment **II** of Fig. S4B in both wt and bp versions) was prepared by standard PCR and cloning methods from the plasmid encoding P4-P6-24 (nt 102-237 terminating with a cyclic phosphate, in both wt and bp versions).[25] All oligonucleotides, transcripts, and ligation products were purified by denaturing PAGE. [26,27]

Procedures for Preparation of RNA-DNA Conjugates. As shown in Fig. S4A, 10-mer and 20-mer DNA oligonucleotides with a 5'-diol were prepared by solid-phase synthesis using a modified thymidine phosphoramidite. After $NaIO_4$ oxidation of the 1,2-diol, the resulting 5'-aldehyde DNA was covalently joined with 2'-amino-2'-deoxy-RNA by reductive amination with $NaCNBH_3$. The amino-derivatized RNA oligonucleotides (fragments **I** and/or **III** in Fig. S4B) were prepared by solid-phase synthesis using 2'-amino-2'-deoxyribonucleoside phosphoramidites. The synthetic DNA and RNA phosphoramidites were prepared as described elsewhere (C.V.M. and S.K.S., manuscript in preparation). For the 10-bp and 20-bp DNA constraints, the DNA sequences attached at U107 and C240 were as follows (each 5'-T was modified as shown in Fig. S4A): 10-mer DNA at U107, 5'-TGGACGGCGA-3'; 10-mer DNA at C240, 5'-TCGCCGTCCA-3'; 20-mer DNA at U107, 5'-TGGAGAGCGGTGGACGGCGA-3'; 20-mer DNA at C240, 5'-TCGCCGTCCACCGCTCTCCA-3'.

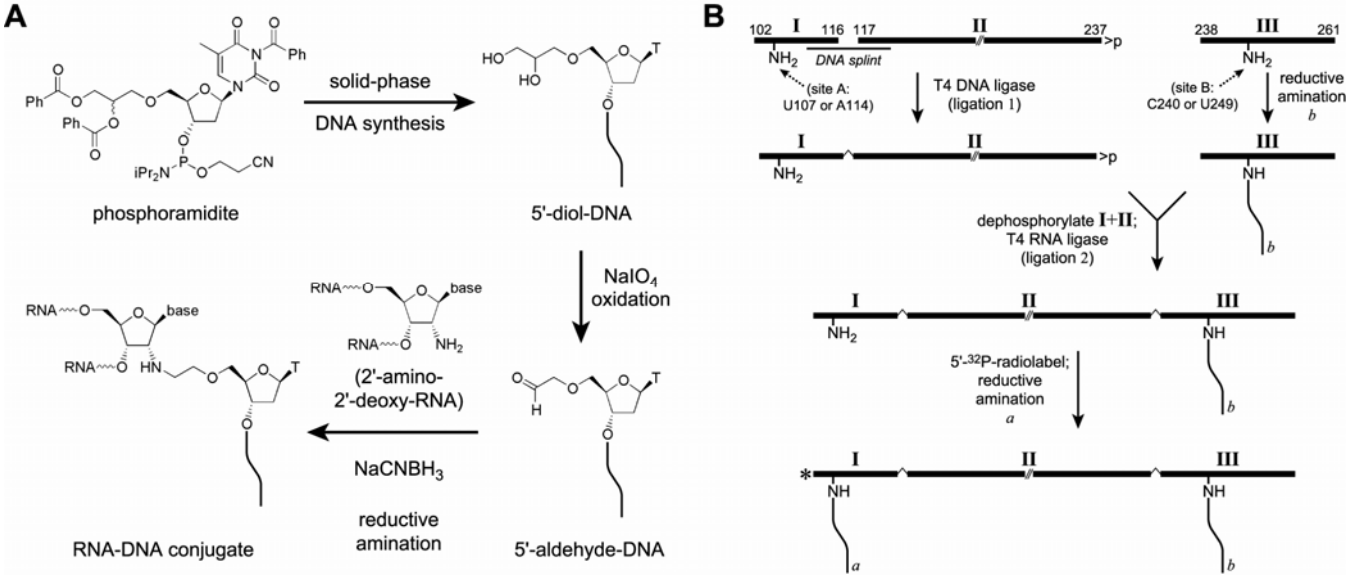

Figure S4. Strategy for preparation of RNA-DNA conjugates. (A) General approach involving solid-phase synthesis of 5'-diol DNA, oxidation to 5'-aldehyde DNA, and reductive amination with 2'-amino-2'-deoxy-RNA. (B) Strategy to assemble the 160-nt P4-P6 RNA (nt 102-261) with two DNA strands attached at sites A and B.

The procedure for synthesizing the P4-P6 RNA-DNA conjugates by reductive amination is shown in Fig. S4B. The two RNA ligation events are denoted "ligation 1" (joining fragments **I** and **II**) and

"ligation 2" (joining fragments **I**+**II** and **III**). Ligation 1 used T4 DNA ligase with a DNA splint to hold together the two RNA fragments.[21] Ligation 2 used T4 RNA ligase and no DNA splint,[28] with the RNA secondary structure holding the two RNA fragments together.[29] The 2',3'-cyclic phosphate of fragment **II** was removed with T4 polynucleotide kinase (PNK) prior to ligation 2. The two reductive amination reactions to join DNA and RNA are denoted "reductive amination *a*" and "reductive amination *b*". When a DNA strand was placed at site A only, fragments **II**+**III** were synthesized as a single transcript,[22] obviating the need for ligation 2. All 5'-monophosphorylation reactions (using T4 PNK and either unradiolabeled ATP or γ-^{32}P-ATP) were performed by standard procedures.

Ligation 1. Oligoribonucleotide **I** (2.0 nmol, with reductive amination site A) was mixed with transcript **II** (2.8 nmol) and a DNA splint (3.6 nmol of sequence complementary to P4-P6 nucleotides 104–154) [21] in a total volume of 100 µL containing 5 mM Tris, pH 7.5, and 0.1 mM EDTA. The sample was annealed by heating at 95 °C for 3 min and cooling on ice for 5 min. To the sample was added 10× ligation buffer and T4 DNA ligase (C-terminal his_6-tagged), providing a total volume of 125 µL containing 50 mM Tris, pH 8.0, 10 mM $MgCl_2$, 7.5 mM DTT, and 1 mM ATP. The sample was incubated at 37 °C for 4.5 h then quenched with 125 µL of stop solution, which contained 80% formamide, 1× TB [89 mM each Tris and boric acid, pH 8.3], and 50 mM EDTA. The ligation product **I**–**II** was purified by 12% denaturing PAGE. The yield was typically 1.4–1.6 nmol.

$NaIO_4$ oxidation of 5'-diol-DNA to 5'-aldehyde-DNA. To a solution of 5'-diol-DNA (6 nmol) in 200 mM sodium phosphate buffer, pH 7.0, was added $NaIO_4$ (1000× relative to DNA, added from an 0.2 M aqueous stock solution). The 50-µL sample was incubated at room temperature, and excess $NaIO_4$ was removed with a Sephadex G-25 mini spin column (Amersham). The eluted material was evaporated to dryness on a SpeedVac, and the 5'-aldehyde-DNA (assumed 6 nmol) was used immediately.

Reductive amination b. Oligoribonucleotide **III** (5 nmol) was mixed with 5'-aldehyde-DNA (6 nmol) in a total volume of 100 µL containing 100 mM sodium acetate, pH 5.0, 25 mM $NiCl_2$, and 10 mM $NaCNBH_3$. The $NiCl_2$ and $NaCNBH_3$ were each added from 0.1 M aqueous stock solutions and were added last. The slightly turbid solution was incubated at 37–45 °C for 16 h; the incubation temperature was optimized for each 5'-aldehyde-DNA sequence. The colorless solution was diluted to 300 µL with water; the nucleic acids were precipitated with ethanol; and the product was purified by 12% or 20% denaturing PAGE. A typical yield was 1.5-2.0 nmol of the reductive amination product.

Ligation 2. (*i*) Dephosphorylation of **I**–**II**: A portion of **I**–**II** from the first ligation reaction (500 pmol) was dephosphorylated in a total volume of 25 µL containing 100 mM sodium phosphate, pH 6.0, 10 mM $MgCl_2$, 5 mM DTT and 25 U T4 PNK (Fermentas). After incubation at 37 °C for 20 h, the sample was diluted to 100 µL with water, and the nucleic acids were precipitated with ethanol. (*ii*) Ligation of **I**–**II** with **III**: The dephosphorylated **I**–**II** (500 pmol) and 5'-monophosphorylated **III** (600 pmol; with the 5'-phosphate from treatment with T4 PNK and ATP after the reductive amination *b* step) were mixed in a total volume of 13 µL containing 5 mM Tris, pH 7.5, and 0.1 mM EDTA. The sample was annealed by heating at 95 °C for 3 min and cooling on ice for 5 min. To the sample was added 10× ligation buffer and T4 RNA ligase, providing a total volume of 20 µL containing 50 mM Tris, pH 7.5, 10 mM $MgCl_2$, 10 mM DTT, 1 mM ATP, and 80 U T4 RNA ligase (Fermentas). The sample was incubated at 37 °C for 5.5 h then quenched with 30 µL of stop solution containing 80% formamide, 1× TB, and 50 mM EDTA. The ligation product **I**–**II**–**III** was purified by 12% denaturing PAGE. The yield was typically 25–185 pmol.

Reductive amination a. A portion of 5'-^{32}P-radiolabeled **I**–**II**–**III** (5 pmol) was mixed with a disruptor DNA oligonucleotide (500 pmol of sequence complementary to P4-P6 nucleotides 175–225) in a total volume of 4 µL containing 5 mM Tris, pH 7.5, and 0.1 mM EDTA. The sample was annealed by heating at 95 °C for 3 min and cooling on ice for 5 min. This sample was mixed with 5'-aldehyde-DNA (1 nmol) in a total volume of 10 µL containing 100 mM sodium acetate, pH 5.0, 10 mM sodium dihydrogen phosphate as a general phosphatase inhibitor, 25 mM $NiCl_2$, and 10 mM $NaCNBH_3$. The $NiCl_2$ and $NaCNBH_3$ were each added from 0.1 M aqueous stock solutions and were added last. The slightly turbid solution was incubated at 37 °C for 16 h. The clear solution was mixed with 15 µL of stop solution and the product was purified by 12% denaturing PAGE. A typical yield was 40–80% of the radiolabeled **I**–**II**–**III** derivatized with the second DNA strand.

For RNA-DNA conjugates with a DNA strand at site A only, nearly the same procedure was used. For ligation 1, 4.0 nmol of oligoribonucleotide **I**, 7.2 nmol of transcript **II**+**III**, and 6.0 nmol of DNA splint were annealed in 200 µL and incubated with T4 DNA ligase in 250 µL total volume.

Nondenaturing (Native) Gel Electrophoresis Experiments. Two versions of each P4-P6 RNA were prepared: a wild-type version denoted F for foldable, and an unfolded control version denoted N for nonfoldable. The nonfoldable control RNA has several mutations in the J5/5a region as listed above that disrupt Mg^{2+}-dependent tertiary folding.[23,24] Because this nonfoldable RNA has several artificial base pairs in the J5/5a region, it has previously been termed "BP 5/5a" or "P4-P6-bp".[21,23,24] The gel mobility of each foldable (F) DNA-conjugated RNA was computed relative to the analogous nonfoldable (N) control RNA loaded in an adjacent lane. These types of experiments have been used many times, both by us[21,22,30-33] and by others,[34,35] which strongly validates their application in the present context.

The nondenaturing gel electrophoresis experiments of Fig. 2 were performed as described previously[21,33] with slight modifications. Each 5'-^{32}P-radiolabeled RNA sample (~20–50 fmol; with or without appended DNA strands) was mixed with 10 pmol of carrier RNA (sequence A_{13}) in a total volume of 3 µL containing 5 mM Tris, pH 7.5, 50 mM NaCl, and 0.1 mM EDTA. The sample was annealed by heating at 95 °C for 3 min and cooling on ice for 5 min. To the sample was added 3 µL of 2× native gel loading buffer, which contained 2× TB, 10% glycerol, and twice the final desired concentration of $MgCl_2$ (1× TB contains 89 mM each Tris and boric acid, pH 8.3). The concentration of $MgCl_2$ was adjusted to account for the EDTA present in the annealing buffer. The sample was annealed by heating at 50 °C for 5 min and cooling at 25 °C for 5–10 min, then 5 µL of the annealed sample was loaded into a gel lane. The gels were electrophoresed at 150–200 V and 25 °C for 5–7 h on 8% polyacrylamide gels containing 7 M urea and 1× TB (made using a 40% 29:1 acrylamide:bis-acrylamide stock solution), then dried and exposed to a PhosphorImager screen. As described,[21] the relative gel mobility data were fit to the titration equation $M_{obs} = (M_{low} + M_{high}\bullet K\bullet[Mg^{2+}]^n)/(1 + K\bullet[Mg^{2+}]^n)$, where M_{obs} is the observed relative mobility as a function of $[Mg^{2+}]$; M_{low} and M_{high} are the limiting low and high values of relative mobility; and K and n are the equilibrium constant and Mg^{2+} Hill coefficient for the simple model equation $U + nMg^{2+} = F\bullet nMg^{2+}$ (U = unfolded state, F = folded state). The Mg^{2+} midpoint ($[Mg^{2+}]_{1/2}$ value) is $K^{-1/n}$. Values of ΔΔG° were calculated as described,[21] with ΔG° for each RNA equal to $+nRT\bullet\ln [Mg^{2+}]_{1/2}$ (ΔΔG° is defined as zero for unconstrained P4-P6). Regardless of the fit value of n that was used along with K to compute $[Mg^{2+}]_{1/2}$, $n = 4$ was assumed in calculating all ΔΔG° values, as described.[21] From the data in Fig. 2, fit values of $[Mg^{2+}]_{1/2}$ were 0.74, 0.89 and 11.9 mM; computed values of ΔG° were 0, 0.44, and >6.6 kcal/mol.. Native gel data and titration curves for

comprehensive control experiments on U107-C240 10-bp constrained P4-P6 (analogous to the data of Fig. 2) are shown in Fig. S5.

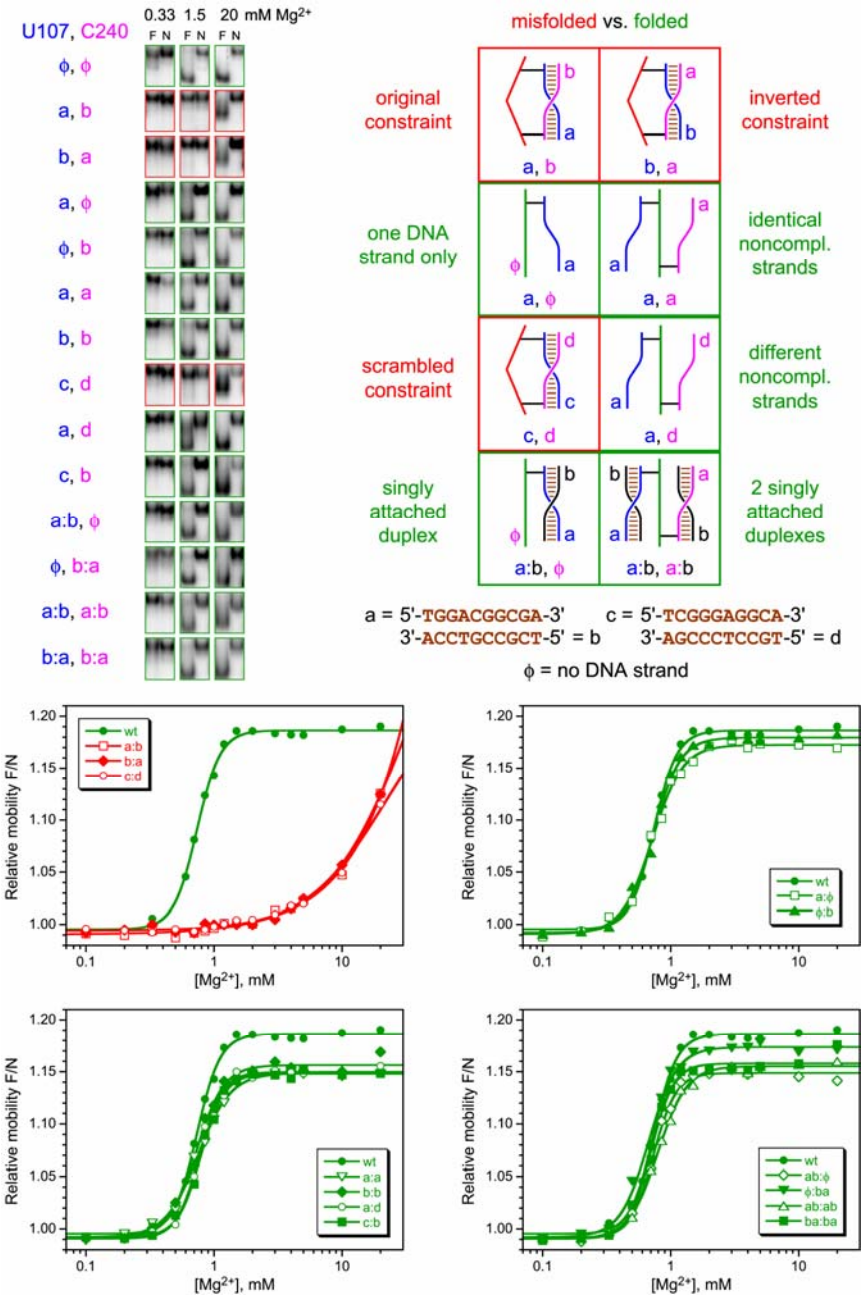

Figure S5. Control nondenaturing gel experiments show that the DNA constraint effect is highly specific (compare gel images and titration curves in Fig. 2). The P4-P6 was derivatized at U107 and C240 with the 10-bp constraint. For all DNA-conjugated RNAs where no constraint effect is expected, a minimal rightward shift in the Mg^{2+} dependence is observed relative to the unconstrained RNA (*green titration curves*). Only for the DNA-conjugated RNAs where a substantial constraint effect is expected is a large rightward shift observed (*red curves*). To prepare the singly attached duplex structures (with a:b and/or b:a), ~100-fold excess of each unattached DNA strand was added.

Dimethyl Sulfate (DMS) Probing Experiments (Fig. S6). For unconstrained P4-P6-wt (F) and P4-P6-bp (N) samples, a 100-µL sample containing 5 pmol of P4-P6-wt or P4-P6-bp in 35 mM Tris, pH 7.5, and the appropriate concentration of $MgCl_2$ was incubated at 50 °C for 5 min then 42 °C for 1 min. To this sample was added 1.25 µL of DMS (1:4 solution in ethanol), and the solution was incubated at 42 °C for 30 min. The reaction was quenched by addition of 25 µL 1 M β-mercaptoethanol followed by 15 µL 3 M NaCl and 12 µg carrier tRNA. The DMS-modified RNA was precipitated with ethanol and dissolved in 10 µL water. For DNA-constrained P4-P6, a 10-µL sample containing 2 pmol of DNA-constrained RNA (A114-U249-10 bp constraint), 5 mM Tris, pH 7.5, 50 mM NaCl, 0.1 mM EDTA, and 10 pmol carrier RNA (sequence A_{13}) was annealed by heating at 95 °C for 3 min and cooling on ice for 5 min. The sample was diluted to 40 µL with final concentrations of 35 mM Tris, pH 7.5 and appropriate $MgCl_2$, then incubated at 50 °C for 5 min and 42 °C for 1 min. To this sample was added 1.25 µL of DMS (1:4 solution in ethanol), and the solution was incubated at 42 °C for 30 min. The reaction was quenched by addition of 25 µL 1 M β-mercaptoethanol followed by 5 µL 3 M NaCl and 4 µg carrier tRNA. The DMS-modified RNA was precipitated with ethanol and dissolved in 10 µL water.

For reverse transcription, a 5-µL sample was prepared containing DMS-modified RNA and 5'-^{32}P-radiolabeled DNA primer in 5 mM Tris, pH 7.5, and 0.1 mM EDTA. The DMS-modified RNA was either 1 pmol (of P4-P6-wt or P4-P6-bp) or 0.5 pmol (of DNA-constrained P4-P6). The DNA primer (3 pmol) was complementary either to P4-P6 nucleotides 195-225 (for P4-P6-wt and DNA-constrained P4-P6) or to nucleotides 241-261 (for P4-P6-wt and P4-P6-bp). Data for P4-P6-wt shown in Fig. S6 used the primer complementary to nt 195-225; data using the other primer were similar. The sample was annealed by heating at 95 °C for 3 min and cooling on ice for 5 min. The sample was brought to 9.5 µL total volume containing 50 mM Tris, pH 8.3, 75 mM KCl, 3 mM $MgCl_2$, 10 mM DTT, and 0.5 mM of each dNTP. An 0.5-µL portion of reverse transcriptase (SuperScript II RNase H^-, Invitrogen, 200 U/µl) was added. The solution was incubated at 42 °C for 90 min then quenched with 10 µL of stop solution. The sample was heated at 95 °C for 3 min and cooled on ice for 5 min before loading onto 12% denaturing PAGE. Dideoxy sequencing ladders (not shown) were generated using P4-P6-wt along with 0.25 mM of one ddNTP and the corresponding dNTP at 0.05 mM.

The Mg^{2+}-dependent intensity of the reverse transcription blockage band corresponding to A152 in each gel lane was normalized to the intensity of the A139 or A171 band, for which DMS modification is nearly independent of $[Mg^{2+}]$. These data were converted to fraction folded by assuming that the limiting value of the A152 band intensity at high $[Mg^{2+}]$ correlates to fully folded RNA (fraction folded = 1.0). The data were fit to $F = K \bullet [Mg^{2+}]^n / (1 + K \bullet [Mg^{2+}]^n)$, where F = fraction folded, K is the equilibrium constant, and n is the Mg^{2+} Hill coefficient.

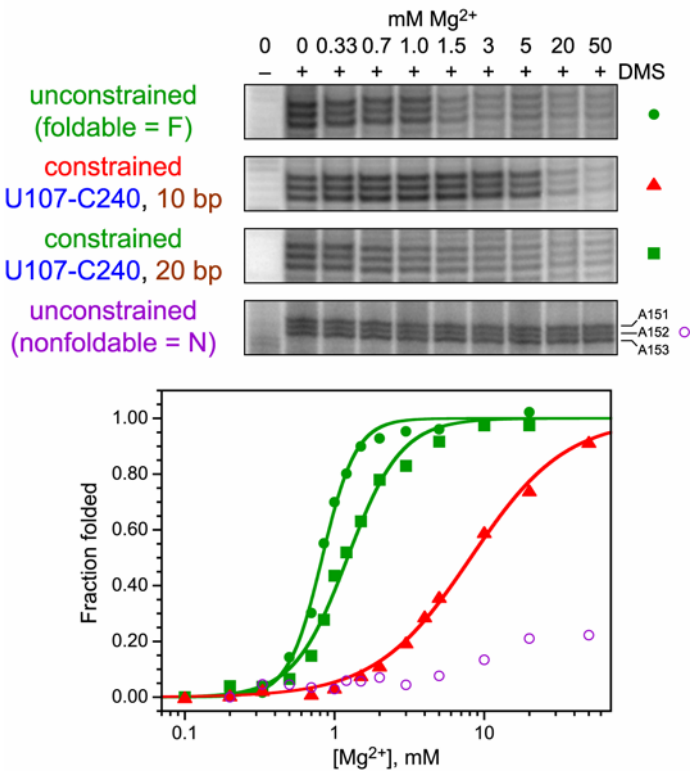

Figure S6. Dimethyl sulfate (DMS) probing to demonstrate the DNA constraint effects. Bands due to reverse transcription blockage at methylated P4-P6 nucleotides A151–A153 correspond to the GAAA tetraloop that is buried (and therefore protected from DMS) upon Mg^{2+}-induced folding.[23] Fit values of $[Mg^{2+}]_{1/2}$ were 0.87, 1.22, and 8.1 mM; computed values of ΔG° were 0, 0.98, and >5.7 kcal/mol. Similar DMS results were obtained for the A114-U249 10-bp constrained RNA (data not shown).

References for Supporting Information

(1) Shih, W. M.; Quispe, J. D.; Joyce, G. F. A 1.7-kilobase single-stranded DNA that folds into a nanoscale octahedron. *Nature* **2004**, *427*, 618-621.
(2) Chen, J.; Seeman, N. C. Synthesis from DNA of a molecule with the connectivity of a cube. *Nature* **1991**, *350*, 631-633.
(3) Zhang, Y.; Seeman, N. C. Construction of a DNA-Truncated Octahedron. *J. Am. Chem. Soc.* **1994**, *116*, 1661-1669.
(4) Mao, C.; Sun, W.; Seeman, N. C. Assembly of Borromean rings from DNA. *Nature* **1997**, *386*, 137-138.
(5) Winfree, E.; Liu, F.; Wenzler, L. A.; Seeman, N. C. Design and self-assembly of two-dimensional DNA crystals. *Nature* **1998**, *394*, 539-544.
(6) Yan, H.; Park, S. H.; Finkelstein, G.; Reif, J. H.; LaBean, T. H. DNA-templated self-assembly of protein arrays and highly conductive nanowires. *Science* **2003**, *301*, 1882-1884.
(7) Keren, K.; Krueger, M.; Gilad, R.; Ben-Yoseph, G.; Sivan, U.; Braun, E. Sequence-specific molecular lithography on single DNA molecules. *Science* **2002**, *297*, 72-75.
(8) Loweth, C. J.; Caldwell, W. B.; Peng, X.; Alivisatos, A. P.; Schultz, P. G. DNA-Based Assembly of Gold Nanocrystals. *Angew. Chem. Int. Ed.* **1999**, *38*, 1808-1812.
(9) Yan, H.; LaBean, T. H.; Feng, L.; Reif, J. H. Directed nucleation assembly of DNA tile complexes for barcode-patterned lattices. *Proc. Natl. Acad. Sci. USA* **2003**, *100*, 8103-8108.
(10) Warner, M. G.; Hutchison, J. E. Linear assemblies of nanoparticles electrostatically organized on DNA scaffolds. *Nature Materials* **2003**, *2*, 272-277.
(11) Zhu, L.; Lukeman, P. S.; Canary, J. W.; Seeman, N. C. Nylon/DNA: Single-stranded DNA with a covalently stitched nylon lining. *J. Am. Chem. Soc.* **2003**, *125*, 10178-10179.

(12) Mao, C.; Sun, W.; Shen, Z.; Seeman, N. C. A nanomechanical device based on the B-Z transition of DNA. *Nature* **1999**, *397*, 144-146.
(13) Yurke, B.; Turberfield, A. J.; Mills, A. P., Jr.; Simmel, F. C.; Neumann, J. L. A DNA-fuelled molecular machine made of DNA. *Nature* **2000**, *406*, 605-608.
(14) Yan, H.; Zhang, X.; Shen, Z.; Seeman, N. C. A robust DNA mechanical device controlled by hybridization topology. *Nature* **2002**, *415*, 62-65.
(15) Li, J. J.; Tan, W. A Single DNA Molecule Nanomotor. *Nano Lett.* **2002**, *2*, 315-318.
(16) Alberti, P.; Mergny, J. L. DNA duplex-quadruplex exchange as the basis for a nanomolecular machine. *Proc. Natl. Acad. Sci. USA* **2003**, *100*, 1569-1573.
(17) Feng, L.; Park, S. H.; Reif, J. H.; Yan, H. A Two-State DNA Lattice Switched by DNA Nanoactuator. *Angew. Chem. Int. Ed.* **2003**, *42*, 4342-4346.
(18) Liao, S.; Seeman, N. C. Translation of DNA signals into polymer assembly instructions. *Science* **2004**, *306*, 2072-2074.
(19) Sherman, W. B.; Seeman, N. C. A Precisely Controlled DNA Biped Walking Device. *Nano Lett.* **2004**, *4*, 1203-1207.
(20) Tinoco, I., Jr.; Bustamante, C. How RNA Folds. *J. Mol. Biol.* **1999**, *293*, 271-281.
(21) Silverman, S. K.; Cech, T. R. Energetics and Cooperativity of Tertiary Hydrogen Bonds in RNA Structure. *Biochemistry* **1999**, *38*, 8691-8702.
(22) Silverman, S. K.; Cech, T. R. RNA Tertiary Folding Monitored by Fluorescence of Covalently Attached Pyrene. *Biochemistry* **1999**, *38*, 14224-14237.
(23) Murphy, F. L.; Cech, T. R. An Independently Folding Domain of RNA Tertiary Structure within the *Tetrahymena* Ribozyme. *Biochemistry* **1993**, *32*, 5291-5300.
(24) Szewczak, A. A.; Cech, T. R. An RNA internal loop acts as a hinge to facilitate ribozyme folding and catalysis. *RNA* **1997**, *3*, 838-849.
(25) Golden, B. L.; Gooding, A. R.; Podell, E. R.; Cech, T. R. X-ray crystallography of large RNAs: Heavy-atom derivatives by RNA engineering. *RNA* **1996**, *2*, 1295-1305.
(26) Flynn-Charlebois, A.; Wang, Y.; Prior, T. K.; Rashid, I.; Hoadley, K. A.; Coppins, R. L.; Wolf, A. C.; Silverman, S. K. Deoxyribozymes with 2'-5' RNA Ligase Activity. *J. Am. Chem. Soc.* **2003**, *125*, 2444-2454.
(27) Wang, Y.; Silverman, S. K. Characterization of Deoxyribozymes That Synthesize Branched RNA. *Biochemistry* **2003**, *42*, 15252-15263.
(28) Bain, J. D.; Switzer, C. Regioselective ligation of oligoribonucleotides using DNA splints. *Nucleic Acids Res.* **1992**, *20*, 4372.
(29) Pan, T.; Gutell, R. R.; Uhlenbeck, O. C. Folding of circularly permuted transfer RNAs. *Science* **1991**, *254*, 1361-1364.
(30) Silverman, S. K.; Zheng, M.; Wu, M.; Tinoco, I., Jr.; Cech, T. R. Quantifying the energetic interplay of RNA tertiary and secondary structure interactions. *RNA* **1999**, *5*, 1665-1674.
(31) Silverman, S. K.; Deras, M. L.; Woodson, S. A.; Scaringe, S. A.; Cech, T. R. Multiple Folding Pathways for the P4-P6 RNA Domain. *Biochemistry* **2000**, *39*, 12465-12475.
(32) Silverman, S. K.; Cech, T. R. An Early Transition State for Folding of the P4-P6 RNA Domain. *RNA* **2001**, *7*, 161-166.
(33) Young, B. T.; Silverman, S. K. The GAAA tetraloop-receptor interaction contributes differentially to folding thermodynamics and kinetics for the P4-P6 RNA domain. *Biochemistry* **2002**, *41*, 12271-12276.
(34) Doherty, E. A.; Batey, R. T.; Masquida, B.; Doudna, J. A. A universal mode of helix packing in RNA. *Nature Struct. Biol.* **2001**, *8*, 339-343.
(35) Matsumura, S.; Ikawa, Y.; Inoue, T. Biochemical characterization of the kink-turn RNA motif. *Nucleic Acids Res.* **2003**, *31*, 5544-5551.